Journal of Photochemistry and Photobiology A: Chemistry 200 (2008) 445–450

Contents lists available at ScienceDirect

Journal of Photochemistry and Photobiology A: Chemistry

journal homepage: www.elsevier.com/locate/jphotochem

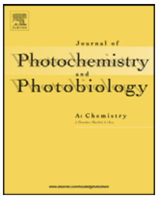

UV–vis photodegradation of dyes in the presence of colloidal Q-CdS

M. Hamity, R.H. Lema*, C.A. Suchetti, H.E. Gsponer

Departamento de Química, Facultad de Ciencias Exactas Fisicoquímicas y Naturales, Universidad Nacional de Río Cuarto, Ruta 36 Km 601, 5800 Río Cuarto, Argentina

ARTICLE INFO

Article history:
Received 7 May 2008
Received in revised form 19 August 2008
Accepted 19 September 2008
Available online 2 October 2008

Keywords:
Nanoscience
Q-CdS
Safranin-O
Orange II
Fluorescence

ABSTRACT

The interaction of the dyes Safranin-O (SO) and Orange II (OII) with aqueous colloidal Q-CdS clusters, which emit single fluorescence bands with maximum wavelengths at 481 nm (excitonic band) or 559 nm (trapped band), has been studied. This was carried out by monitoring both the photodegradation of the dye in the presence of the clusters and the quenching of the clusters fluorescence by the dyes. The photolysis experiments were carried out by excitation either at 520 nm (the wavelength at which the dyes, but not the clusters absorb light) or at 350 nm (the wavelength at which the clusters strongly absorb light, and the dyes have absorbance minima). At 520 nm, photodegradation of SO could be observed, which follows a first-order kinetics (for trapped-band clusters) and a second-order kinetics (for excitonic-band clusters). For the excitation wavelength of 350 nm, photodegradation of either of the dyes could not be observed. The Stern–Volmer plots for the quenching of the excitonic band-clusters fluorescence by SO show an upward curvature, pointing to the occurrence of more than one species acting as the fluorescence quencher, whereas the Stern–Volmer plots for the quenching of the trapped band-clusters fluorescence by SO are linear, indicating that only one species acts as a fluorescence quencher. Lambert–Beer type plots (absorbance vs. concentration) are linear for SO in water and in trapped band-clusters solutions, but a similar study of SO in excitonic band-clusters solution show the occurrence of a new band, which can be assigned to a ground-state dimer of the dye. The latter can be used to explain both the upward curvature of the Stern–Volmer plots and the second-order kinetics observed for SO photodegradation in the SO-excitonic band-clusters system. The Stern–Volmer plots for the quenching of both fluorescence bands by OII are linear.

1. Introduction

Scientific and technological applications of nanomaterials are currently of great interest and their uses are rapidly growing [1–3]. In particular, semiconductor nanoparticles (SC-NPs) show characteristic physicochemical properties that are different from those of both the bulk and the molecular substance, these properties facilitate their use in diverse fields, such as in optoelectronics [4], for solar-energy conversion [5,6] and in photocatalysis [7].

A process that is common to the latter two fields concerns the interaction between SC-NPs and some dye present in the aqueous solution and/or adsorbed onto the NP surface. For solar-energy conversion, a number of dyes are used as photosensitizers for wide band-gap (UV-absorbing) semiconductors; to extend the wavelengths absorbed by the system to the visible range [8–10].

Moreover, the textile industry uses many dyes, which enter the wastewater as pollutants and therefore must be degraded, for which purpose SC-NPs promise to be very useful [11–17]. Among the dyes that are very commonly used in the textile industry, chemicals for which photodegradation using SCs is currently under investigation, are the sulfonated azo dyes [18–20] and the phenazine dyes [21].

Azo dyes comprise the largest class of textile dyes in industrial use [22]. The sulfonated azo dye Orange II (4-(2-hydroxy-1-naphthylazo) benzene sulfonic acid sodium salt, Scheme 1) is widely used in the dyeing of textiles, food, and cosmetics. For this reason, there have been several publications dealing with its degradability using different methods for wastewaters [23–25].

The phenazine dye Safranin-O (3,7-diamino-2,8-dimethyl-5 phenylphenazinium chloride, Scheme 2), similar to other phenazine dyes, has been extensively used as a photosensitizer in energy-transfer and electron-transfer reactions [26], in addition to being used as a sensitizer in visible-light photopolymerization [27]. Safranin-O has been found to act as either a photochemical oxidant or a reductant [28], and its spectroscopic and photophysical properties in aqueous solutions are well documented [29,30].

A study of the interaction between colloidal CdS-NPs in an aqueous solution and two dyes, the anionic dye Orange II (OII) and the cationic dye Safranin-O (SO), is presented herein. The experiments have been carried out by monitoring both the photodegradation of

---

* Corresponding author. Tel.: +54 358 4676538 fax: +54 358 4676233.
E-mail address: rlema@exa.unrc.edu.ar (R.H. Lema).

1010-6030/$ – see front matter © 2008 Elsevier B.V. All rights reserved.
doi:10.1016/j.jphotochem.2008.09.010

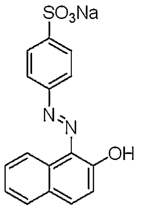

Scheme 1. Orange II.

the dye in the presence of Q-CdS-NPs and the quenching of the NP fluorescence by the dyes.

The samples of colloidal CdS-NPs (Q-CdS) are prepared as described in a previous work [31]. They emit characteristic single fluorescence bands, identified as the excitonic band and the trapped band, and therefore, the particles have been named respectively, as excitonic-band nanoparticles (NP_{EB}) and trapped-band nanoparticles (NP_{TB}).

2. Experimental

2.1. Chemicals

Cadmium sulfate (Mallinckrodt), sodium polyphosphate, sodium sulfide, and Orange II (Merck) were of analytical grade and they were used without further purification. Safranin-O (Aldrich) was recrystallized twice from methanol before use.

2.2. Preparation of Q-CdS colloids

Samples of colloidal Q-CdS, which emitted single fluorescence bands with maximum wavelength at 481 nm (excitonic band) or 559 nm (trapped band), have been prepared. The excitation and emission spectra of Q-CdS are shown in Fig. 1. The samples were prepared as described in a previous work [31]. The following is a brief explanation of the experimental procedure.

An aqueous solution of $CdSO_4$ containing sodium polyphosphate as stabilizer, was de-oxygenated by nitrogen bubbling for 30 min. Subsequently, a specific quantity of $H_2S_{(g)}$ was added, depending on the clusters to be prepared (see Table 1), while keeping the vessel hermetically closed. In nearly 2 min, the solution became pale yellow and, after 10 min, the excess $H_2S_{(g)}$ was eliminated by nitrogen purging, the pH was adjusted to its final value of pH 10.5. These clusters emitted a very weak fluorescence that was greatly enhanced by the addition of excess Cd^{2+}; therefore, all the samples were prepared with a final Cd^{2+} concentration of 8×10^{-4} M.

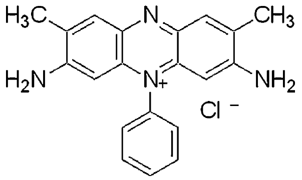

Scheme 2. Safranin-O.

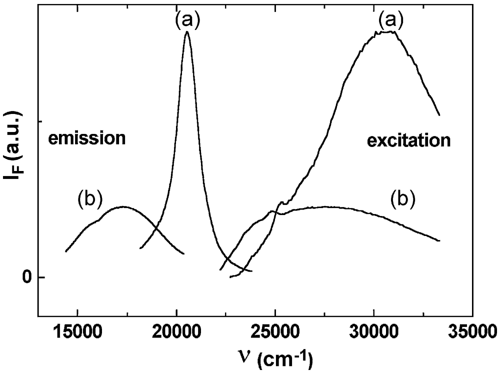

Fig. 1. Fluorescence excitation and emission spectra of the clusters: (a) excitonic band (λ_{max} = 481 nm) and (b) trapped band (λ_{max} = 559 nm).

2.3. Quenching procedures

The quenching experiments were carried out by adding a solution of concentrated quencher in colloidal Q-CdS to the corresponding Q-CdS-clusters solution. Moreover, to detect if there was some interaction between the quenchers and the stabilizing polyphosphate (or the cadmium ion), solutions of the quenchers with polyphosphate and/or $CdSO_4$ at several concentrations were prepared. No detectable effect on the absorbance of the quenchers was observed in these control solutions.

2.4. Photolysis experiments

The photolysis experiments were carried out by preparing solutions with varying concentrations of the dye, in the range of 2×10^{-5} to 5×10^{-5} M, using the corresponding clusters solution (NP_{TB} or NP_{EB}) as the solvent. Irradiation was carried out with a Photon Technology International (PTI) illumination system comprising a 150 W Xe lamp and a monochromator. The irradiation wavelengths were 520 nm or 350 nm and the bandwidth was 8 nm.

NPs are not excited at λ = 520 nm ($\nu \approx$ 19,200 cm^{-1}, see Fig. 1), only the dyes absorb here, whereas at λ = 350 nm ($\nu \approx$ 28,600 cm^{-1}) NPs strongly absorb (see Fig. 1), and the dyes have absorbance minima. The samples to be irradiated with λ = 350 nm wavelength, were prepared to obtain a dye absorbance that was:

For SO: $A_{SO} < 0.01 A_{NPs}$.
For OII: $A_{OII} < 0.1 A_{NPs}$.

Photolysis experiments at 520 nm with aqueous solutions of the dyes in the absence of the clusters have additionally been carried out.

2.5. Lambert–Beer experiments

To determine the occurrence of possible interactions between the dye molecules and the Q-CdS clusters or associations between the dye molecules in the aqueous solution or in Q-CdS clusters solution, we have carried out Lambert–Beer law experiments at variable dye concentrations, using either water or the corresponding clusters solution (NP_{TB} or NP_{EB}) as the solvent. Starting with the corresponding solvent in both the sample and reference cell, a concentrated solution of the dye in the solvent was added with a microliter syringe to obtain a given dye concentration and magnetically stirred until a stable absorbance reading was obtained, which taked less than 5 min.

2.6. Apparatus

UV–vis absorption measurements were conducted with a Hewlett-Packard HP-8453 Diode-Array Spectrophotometer.

Fluorescence lifetimes were measured using the time-correlated single-photon counting technique on an Edinburgh Analytical Instruments OB900 fluorometer.

Table 1
Experimental conditions for the preparation of the clusters and their fluorescence characteristics.

Band	$[CdSO_4]$i	$[(NaPO_3)_6]$	pHi	$[H_2S]/[Cd^{2+}]$i	τ_1	τ_2	τ_3	$(Rel)_1$%	$(Rel)_2$%	$(Rel)_3$%
481 nm	2×10^{-4} M	2×10^{-4} M	8.7	Excess H_2S	6.7	53	350	25	44	31
559 nm	2×10^{-4} M	2×10^{-4} M	10.5	1/1	3	70	385	8.4	31.6	60

The irradiation system for photolysis experiments was a Photon Technology International (PTI) illumination system comprising a 150 W Xe lamp and a monochromator.

3. Results and discussion

A study of the possible photodegradation of the dyes SO and OII in the presence of CdS-NPs, which emit single fluorescence bands with the maximum wavelengths at 481 nm (excitonic band) or 559 nm (trapped band) is presented in this article.

The photolysis experiments have been carried out for all the dye-NP systems using (i) exciting wavelengths at which the NPs strongly absorb light and the dyes have absorbance minima and (ii) wavelengths at which the dyes absorb light whereas the NPs do not.

The effects produced by the dyes on the fluorescence bands of both types of Q-CdS clusters have also been studied.

3.1. Photolysis of the dyes in the presence of CdS-NPs

During the photolysis experiments, using exciting wavelength at 520 nm, which is absorbed by the dye (SO or OII) and not by the CdS-NPs, degradation of SO was observed, in the presence of both kinds of NPs: those emitting the excitonic and those emitting the trapped bands. For OII, however, degradation could not be detected in the presence of any of the bands.

On the contrary, photodegradation of the dyes could neither be observed by excitation of the CdS-NPs with a wavelength of 350 nm, where the absorption of the dyes is negligible, nor when the aqueous solutions of the dyes were excited at 520 nm in the absence of NPs. We have also monitored the absorption band of NPs, to detect possible changes in the clusters during the photolysis experiments with λ = 350 nm, and we could not observe any change.

For the photolysis of SO in the presence of the CdS-NPs that emit the excitonic band, a second-order kinetics was observed with SO concentration, as shown in Fig. 2, whereas for the photolysis of the same dye in the presence of the CdS-NPs emitting the trapped band, a first-order kinetics was observed (Fig. 3). The values of the corresponding pseudo-rate constants are provided in Table 2.

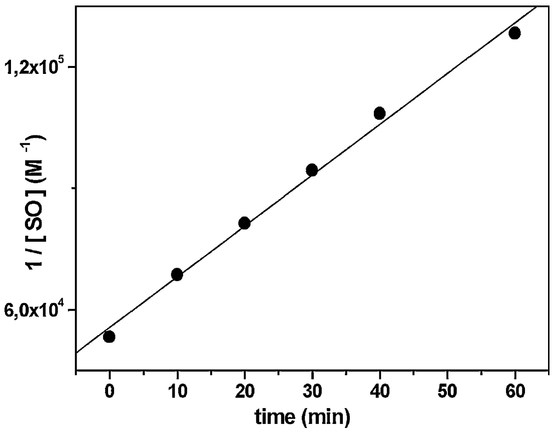

Fig. 2. Second-order plot for the kinetics of photodegradation of SO in CdS-NP_{EB} solution. Initial concentration of SO = 1.9×10^{-5} M.

The results obtained for the photodegradation of the dyes can be justified through a reduction-potential diagram, as depicted in Fig. 4. The conduction band (CB) potential for the bulk CdS (powder) is nearly −1 V vs. normal hydrogen electrode, (NHE), whereas the corresponding valence band (VB) potential is nearly 1.5 V vs. NHE, yielding a band gap of nearly 2.5 V [19]. The reduction potentials for the dyes, from previous reports, are −1.21 V for the singlet excited state of SO [32] and −1.25 V for the singlet excited state of OII [19]. These values indicate that the excited state of both dyes can release electrons to the conduction band of the CdS powder (−1 V vs. NHE). This prediction was confirmed practically for the dye OII [19].

In the above experiments, photodegradation of SO, but not of OII, was observed. Instead of CdS powder (band gap ∼ 2.5 V), colloidal CdS-NPs have been used, for which band gaps of ∼2.9 V for the excitonic-band NPs and ∼2.8 V for the trapped-band NPs have been

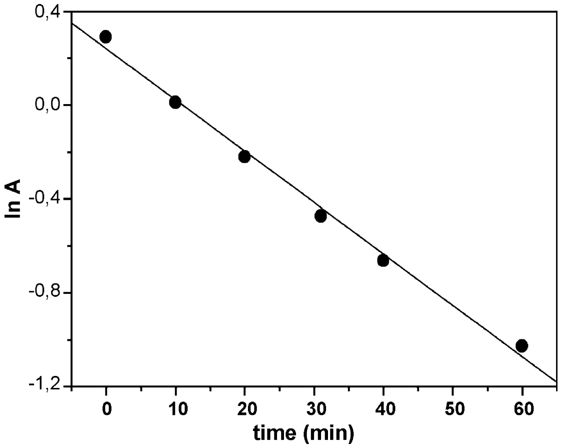

Fig. 3. First-order plot for the kinetics of photodegradation of SO in CdS-NP_{TB} solution. Initial concentration of SO was 4.8×10^{-5} M.

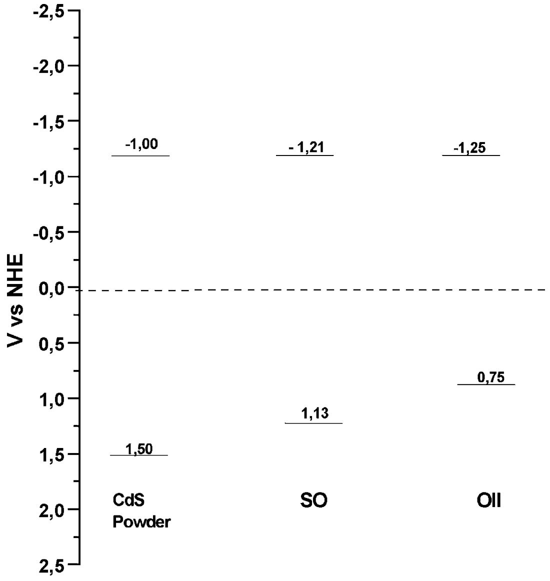

Fig. 4. Reduction potentials of CdS powder, SO and OII.

Table 2
Rate constants and fluorescence-quenching constants for the experimental systems.

Dye	Excitonic band (λ_{em} = 481 nm)		Trapped band (λ_{em} = 559 nm)	
	Dye photodegradation Rate constant	Stern–Volmer constants K_{sv} (M^{-1})	Dye photodegradation Rate constant	Stern–Volmer constants K_{sv} (M^{-1})
Safranin-O	1.2×10^3 M^{-1} min^{-1}	$K_{sv1} = 6.6 \times 10^3$; $K_{sv2} = 3.8 \times 10^8$	2.2×10^{-2} min^{-1}	9.4×10^3
Orange II	–	5.8×10^3	–	3.9×10^3

determined from the onset of the excitation spectra. The shift in the band gap could indicate a correlative shift in the potential of one or both bands (VB and/or CB). This probably would in turn affect the oxidation reactions of both SO and OII, because the reduction potentials for the singlet excited states of both dyes are very close in value (SO ≈ −1.21 V and OII ≈ −1.25 V). However, SO undergoes photodegradation whereas OII does not.

A probable explanation for these results could be provided as follows: since the excited singlet-state lifetime of the dye is very short, the electron transfer from the dye to the NP-conduction band requires that the dye remain adsorbed onto the NP surface at the time of photoexcitation. The pH value of the colloidal CdS-NP solution is nearly 10 and, under these conditions, CdS-NPs have an excess negative surface charge. The anionic dye OII would be electrostatically repelled by this surface, but the cationic dye SO would be electrostatically attracted and would be adsorbed onto the NP surface, thus supporting the oxidation of the SO photoexcited singlet state.

The effect of pH on the photodegradation of OII by ZnO was observed by Daneshvar et al. [23], they determined an optimum pH of nearly 7.5 and a lowering of the photodegradation of the dye at higher pH. This effect was attributed to the negative charge of the dye as well as the ZnO nanopowder. At pH lower than 7, photocorrosion of ZnO takes place and the photodegradation of the dye is less efficient. In our working group, we have observed an appreciable corrosion effect for CdS colloids at pH values lower than nearly 8. Gupta et. al. [21] have observed a noticeable rise in the photodegradation of Safranin with TiO_2 at high pH values, attributed to an increment of the negative charge on the TiO_2 photocatalyst.

In the photolysis experiments, a remarkable difference was observed between the kinetic behaviors of the SO-trapped-band NP system, which is of the first order, and the SO-excitonic-band NP system, which is of the second order (Fig. 3 and Fig. 2, respectively) with respect to the SO concentration. To determine the source of this difference, UV–vis spectra were obtained under variable SO concentrations, for the following systems: SO, SO-trapped-band NPs, and SO-excitonic-band NPs in water.

For the SO and SO-trapped-band NPs systems, a linear dependence of absorbance (measured on the characteristic absorption band of SO) with molar concentration of SO was observed. However, for the SO-excitonic-band NP system, a new blue-shifted absorption band was observed, which absorbance increased with the increase in SO molar concentration (Fig. 5). Many dyes show this characteristic behavior, which may be due to the formation of molecular associations such as dimers or higher aggregates, when the dye concentration increases [33]. From the results obtained, it can be concluded that, even though the dye SO can be adsorbed onto the surfaces of both, NP_{TB} and NP_{EB} nanoparticles, the formation of dimers is evident only for NP_{EB}.

The results of the photodegradation kinetics for the SO-NP_{EB} system can be explained with reference to a mechanistic scheme that assumes initially the formation of a dimer of SO that is adsorbed on the NP surface $\{(SO)_{2,ad}\}$, and this process may be represented as follows:

$$SO_{aq} + NP_{EB} \leftrightarrows SO_{ad} \tag{1}$$

$$SO_{aq} + SO_{ad} \leftrightarrows (SO)_{2,ad} \tag{2}$$

$$(SO)_{2,ad} + h\nu \rightarrow (SO)_{2,ad}{}^{*} \tag{3}$$

$$(SO)_{2,ad}{}^{*} \rightarrow (SO)_{2,ad} \tag{4}$$

$$(SO)_{2,ad}{}^{*} \rightarrow P \tag{5}$$

where (P) indicates the photodegradation products. From steps (1) and (2), which account for the adsorption of the dye molecules and the formation of dimers on the NP surface, the following equation is obtained:

$$[(SO)_{2,ad}] = K_1 K_2 [NP_{EB}][SO_{aq}]^2 \tag{6}$$

Steps (4) and (5) represent the deactivation and the photochemical reaction of the adsorbed dimers, respectively, the rate of the photochemical reaction being expressed as:

$$\frac{-d[(SO)_{2,ad}]}{dt} = \phi I_A \propto \phi\varepsilon[(SO)_{2,ad}] \tag{7}$$

where ϕ is the quantum yield for step (5), I_A is the intensity of the light absorbed by the dimer and ε is the corresponding extinction coefficient. Eq. (7) holds good for low absorbances of the dye at the excitation wavelength, in which case the quantum yield is obtained from the following equation:

$$\phi = k_5/(k_4 + k_5) \tag{8}$$

where k_4 and k_5 are the rate constants for steps (4) and (5), respectively. From Eqs. (6) and (7) the following relation for the kinetics of photodegradation of SO in the presence of NP_{EB} is obtained::

$$\frac{-d[(SO)_{2,ad}]}{dt} \propto \phi\varepsilon K_1 K_2 [NP_{EB}]\,[SO_{aq}]^2 = k[SO_{aq}]^2 \tag{9}$$

which shows a second-order dependence on the aqueous concentration of SO.

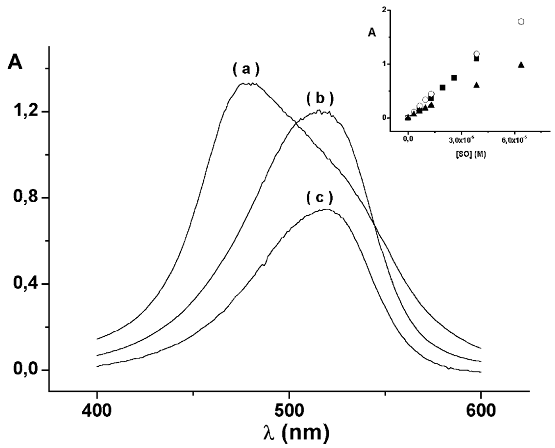

Fig. 5. Absorption spectra of SO at pH 10 in solutions containing: (a) NP_{EB}, [SO] = 6.4×10^{-5} M; (b) NP_{TB}, [SO] = 3.8×10^{-5} M and (c) solvent (water) without NPs, [SO] = 2.6×10^{-5} M. (Inset) Lambert–Beer plots for SO (A_{SO} at λ = 520 nm vs. [SO]) at pH 10 in solutions containing NP_{EB} (▲), NP_{TB} (○), and solvent (water) without NPs (■).

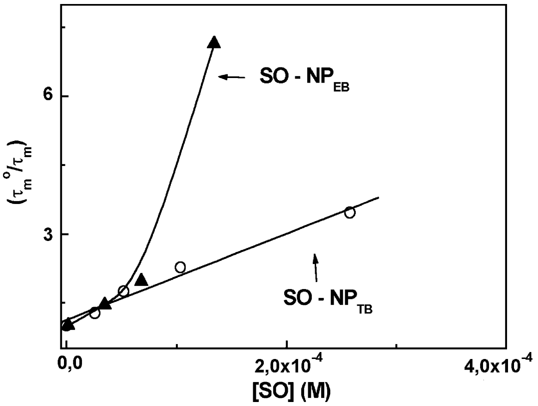

Fig. 6. Stern–Volmer plots for the quenching of the two fluorescence bands by SO: excitonic band (▲) and trapped band (○).

For the photodegradation of SO in the presence of trapped-band NPs, the kinetics results can be explained through a mechanistic scheme which is similar to the one provided above, except the dimer-formation step (2)

$$SO_{aq} + NP_{TB} \leftrightarrows SO_{ad} \tag{1b}$$

$$SO_{ad} + h\nu \rightarrow SO_{ad}{}^* \tag{3b}$$

$$SO_{ad}{}^* \rightarrow SO_{ad} \tag{4b}$$

$$SO_{ad}{}^* \rightarrow P \tag{5b}$$

where (NP_{TB}) indicates the trapped-band NPs. According to this scheme, Eq. (9) changes to

$$\frac{-d[SO_{ad}]}{dt} \propto \phi\varepsilon K_{1b}[NP_{TB}][SO_{aq}] = k'[SO_{aq}] \tag{9b}$$

which is of the first order with respect to the aqueous SO concentration. The values of the rate constants for Eq. (9) and Eq. (9b) are presented in Table 2.

3.2. *Quenching of the fluorescence from CdS-NPs by SO and OII*

The quenching of the fluorescence from NPs emitting both, in the excitonic band and the trapped band has been studied. The Stern–Volmer plots for the quenching of the trapped band by SO are linear, whereas those corresponding to the quenching of the excitonic-band fluorescence by the same dye show an upward curvature, as shown in Fig. 6.

The Stern–Volmer plots for the quenching of the fluorescence bands from both the excitonic-band NPs and the trapped-band NPs with OII are linear, as shown in Fig. 7. The values of the Stern–Volmer constants (K_{SV}), obtained from the slopes in the linear Stern–Volmer plots, are listed in Table 2.

To explain the results observed for fluorophores with multiple luminescent states, such as the SC-NPs, a multisite quenching model must be used [34–36]. Our results show dynamic quenching in all the experiments, and so the application of the model to fit our experimental data requires the use of preexponential factor-weighted mean lifetimes, defined by the following equation:

$$\tau_m = \frac{\sum_i \alpha_i \tau_i}{\sum_i \alpha_i} \tag{10}$$

where $\boldsymbol{\alpha_i}$ is the preexponential factor for each decay component.

Figs. 6 and 7 show plots of τ_m°/τ_m vs. [Q], for which the τ_m values have been calculated from the luminescence-decay data using Eq. (10) and [Q] is the dye concentration in the aqueous solution. Moreover, τ_m° and τ_m are the mean lifetimes in the absence and presence of quencher, respectively.

A probable quenching mechanism, which can account for the experimental results shown in Figs. 6 and 7, is provided below, beginning with the excitation of Q-CdS-NP:

$$NP + h\nu \rightarrow NP^* \quad (\equiv h^+, e^-) \tag{11}$$

Radiative recombination:

$$(h^+, e^-) \xrightarrow{k_F} NP + h\nu' \tag{12}$$

Non-radiative pathway:

$$(h^+, e^-) \xrightarrow{k_D} NP \tag{13}$$

The quenching process for the quencher dye SO, which is adsorbed onto the NP surface, occurs through the transfer of one electron from the dye in its ground singlet state to a hole in the valence band of the CdS-NP {$NP^*(h^+)$}. For NP_{EB}, two distinct quenching processes are possible: quenching by the adsorbed monomer and quenching by the adsorbed dimer

$$NP_{EB}{}^*(h^+) + SO_{ad} \xrightarrow{k_{QM}} \text{quenching} \tag{14}$$

$$NP_{EB}{}^*(h^+) + (SO)_{2,ad} \xrightarrow{k_{QD}} \text{quenching} \tag{15}$$

where k_{QM} and k_{QD} indicate the quenching rate constants for the monomer and dimer, respectively. The corresponding Stern–Volmer equation is

$$\frac{\tau_m^\circ}{\tau_m} = 1 + K_{SVM}[SO_{ad}] + K_{SVD}[(SO)_{2,ad}] \tag{16}$$

This equation allows for the adsorption of SO onto the CdS-NP surface, both as a monomer {$(SO)_{ad}$} and as a dimer {$(SO)_{2,ad}$}. To express it as a function of aqueous solution concentrations, Eqs. (1) and (2) and the corresponding adsorption constants for the quencher are used, and the following equation is obtained:

$$\frac{\tau_m^\circ}{\tau_m} = 1 + K_{SV1}[SO_{aq}] + K_{SV2}[SO_{aq}]^2 \tag{17}$$

This accounts for the upward curvature in the Stern–Volmer plot in Fig. 6 for the quenching of NP_{EB} luminescence and corresponds to the SO dimer formation on the NP surface, as evidenced through the absorbance experiments (see above).

For the SO-NP_{TB} system, in which the formation of dimers is not detected through the absorption spectra, only one quenching step

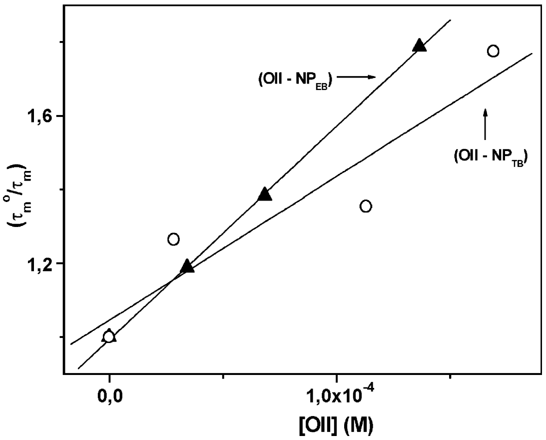

Fig. 7. Stern–Volmer plots for the quenching of the two fluorescence bands by OII: excitonic band (▲) and trapped band (○).

similar to step (14) has been considered:

$$\mathrm{NP_{TB}}^*(\mathrm{h}^+) + \mathrm{SO_{ad}} \xrightarrow{k_Q} \text{quenching} \tag{14b}$$

Thus, the Stern–Volmer equation for this system is represented as:

$$\frac{\tau_\mathrm{m}^\circ}{\tau_\mathrm{m}} = 1 + K_\mathrm{SV}[\mathrm{SO_{aq}}] \tag{17b}$$

which accounts for the linearity of the Stern–Volmer plot in Fig. 6.

For both the systems of Q-CdS nanoparticles with the dye OII, $\mathrm{NP_{TB}}$-OII and $\mathrm{NP_{EB}}$-OII, due to the electrostatic repulsion between the dye and the NPs, both being negatively charged, the quenching process is produced by the interaction of the NPs with the dye in the bulk solution. The Stern–Volmer plots, shown in Fig. 7, are linear and are represented by the equation

$$\frac{\tau_\mathrm{m}^\circ}{\tau_\mathrm{m}} = 1 + K_\mathrm{SV}[\mathrm{OII_{aq}}] \tag{18}$$

The constants K_SV1, K_SV2, and $\mathrm{K_{SV}}$ present in Eqs. (17) and (17b) include terms that account for the adsorption of the dye onto the NP surface, which are not included in the K_SV of Eq. (18). The values of these constants, as obtained for the several systems studied above, are provided in Table 2.

4. Conclusions

The results of the experiments on quenching of the fluorescence of Q-CdS-NPs distinctly point to quenching processes that are mainly dynamic between the valence-band holes (h^+) generated by the photoexcitation of the clusters and the dye in its ground state. The results obtained by the authors in previous studies are coincident with the finding that the process of electron transfer from the quencher to the valence-band holes in the photoexcited NPs is mainly dynamic [31].

Stern–Volmer plots for the quenching of the fluorescence from excitonic-band NPs show an upward curvature, which is indicative of the occurrence of more than one route of interaction between the NPs and SO adsorbed onto the clusters surface. This fact can be related to the second-order kinetics for the photodegradation of SO with excitonic-band NPs. We propose that SO produces a dimeric species adsorbed onto the excitonic-band NP surface, which thus accounts for the observed second-order kinetics of SO, in addition to explaining the upward curvature of the Stern–Volmer plots derived for the quenching process of the excitonic band by SO.

Acknowledgement

This study was supported by a grant from Secretaría de Ciencia y Técnica de la Universidad Nacional de Río Cuarto.

References

[1] T.E. Karakasidis, C.A. Charitidis, Mater. Sci. Eng. C 27 (2007) 1082–1089.
[2] C.G. Granqvist, A. Azens, P. Heszler, L.B. Kish, L. Österlund, Sol. Energy Mater. Sol. Cells 91 (2007) 355–365.
[3] J. Li, C. Chen, J. Zhao, H. Zhu, J. Orthman, Appl. Catal. B: Environ. 37 (2002) 331–338.
[4] K. Dutta, S. De, S.K. De, J. Appl. Phys. 101 (2007) 093711.
[5] P.V. Kamat, J. Phys. Chem. C 111 (2007) 2834–2860.
[6] A.A. Nada, H.A. Hamed, M.H. Barakat, N.R. Mohamed, T.N. Veziroglu, Int. J. Hydrogen Energy 33 (2008) 3264–3269.
[7] M. Matsuoka, M. Kitano, M. Takeuchi, K. Tsujimaru, M. Anpo, J.M. Thomas, Catal. Today 122 (2007) 51–61.
[8] D. Chatterjee, A. Mahata, J. Photochem. Photobiol. A: Chem. 153 (2002) 199–204.
[9] L.M. Peter, J. Photochem. Photobiol. A: Chem. 132 (2000) 1–17.
[10] L.M. Peter, J. Phys. Chem. C 111 (2007) 6601–6612.
[11] N. Strataki, V. Bekiari, E. Stathatos, P. Lianos, J. Photochem. Photobiol. A: Chem. 191 (2007) 13–18.
[12] M. Kositzi, I. Poulios, K. Samara, E. Tsatsaroni, E. Darakas, J. Hazard. Mater. 146 (2007) 680–685.
[13] A.A. Essawy, A. El-Hag Ali, M.S.A. Abdel-Mottaleb, J. Hazard. Mater. 157 (2008) 547–552.
[14] F.D. Mai, C.S. Lu, C.W. Wu, C.H. Huang, J.Y. Chen, C.C. Chen, Sep. Purif. Technol. 62 (2008) 423–436.
[15] M. Saquib, M.A. Tariq, M.M. Haque, M. Muneer, J. Environ. Manage. 88 (2008) 300–306.
[16] K. Dai, H. Chen, T. Peng, D. Ke, H. Yi, Chemosphere 69 (2007) 1361–1367.
[17] A. Syoufian, K. Nakashima, J. Colloid Interface Sci. 317 (2008) 507–512.
[18] T. Papadam, N.P. Xekoukoulotakis, I. Poulios, D. Mantzavinos, J. Photochem. Photobiol. A: Chem. 186 (2007) 308–315.
[19] Y. Bessekhouad, N. Chaoui, M. Trzpit, N. Ghazzal, D. Robert, J.V. Weber, J. Photochem. Photobiol. A: Chem. 183 (2006) 218–224.
[20] C.-H. Wu, Dyes Pigments 77 (2008) 31–38.
[21] V.K. Gupta, R. Jain, A. Mittal, M. Mathur, S. Sikarwar, J. Colloid Interface Sci. 309 (2007) 464–469.
[22] D.R. Waring, G. Hallas, The Chemistry and Application of Dyes, Plenum Press, New York, 1990.
[23] N. Daneshvar, M.H. Rasoulifard, A.R. Khataee, F. Hosseinzadeh, J. Hazard. Mater. 143 (2007) 95–101.
[24] A. Azam, A. Hamid, J. Hazard. Mater. B133 (2006) 167–171.
[25] D. Méndez-Paz, F. Omil, J.M. Lema, Water Res. 39 (2005) 771–778.
[26] S. Saravanan, P. Ramamurthy, J. Chem. Soc., Faraday Trans. 94 (1998) 1675–1679.
[27] M.V. Encinas, A.M. Rufs, M.G. Neumann, C.M. Previtali, Polymer 37 (1996) 1395–1398.
[28] S.G. Bertolotti, C.M. Previtali, J. Photochem. Photobiol. A: Chem. 103 (1997) 115–119.
[29] M.L. Gómez, C.M. Previtali, H.A. Montejano, Spectrochim. Acta Part A 60 (2004) 2433–2439.
[30] S. Nandi, S.C. Bahattacharya, J. Mol. Liquids 89 (2000) 223–231.
[31] C.A. Suchetti, R.H. Lema, M. Hamity, J. Photochem. Photobiol. A: Chem. 169 (2005) 1–8.
[32] S.N. Guha, P.N. Moorthy, J.P. Mittal, Int. J. Radiat. Appl. Instrum. C Radiat. Phys. Chem. 39 (1992) 183–190.
[33] A. Niazi, A. Yazdanipour, J. Ghasemi, M. Kubista, Spectrochim. Acta Part A 65 (2006) 73–78.
[34] M. Klessinger, J. Michl, Excited States and Photochemistry of Organic Molecules, VCH Publishers, New York, 1995.
[35] E.R. Carraway, J.N. Demas, B.A. DeGraaf, J.R. Bacon, Anal. Chem. 63 (1991) 337–342.
[36] C. Landes, C. Burda, M. Braun, M.A. El-Sayed, J. Phys. Chem. B 105 (2001) 2981–2986.